Purple Membrane: Color, Crystallinity, and the Effect of Dimethyl Sulfoxide†

C. Pande,*,‡,§ R. Callender,‡ R. Henderson,∥ and A. Pande⊥,#

Physics Department, City College of The City University of New York, New York, New York 10031, Universitätsspital, Zürich, Switzerland, and MRC Laboratory of Molecular Biology, Cambridge CB2 2QH, U.K.

Received July 29, 1988; Revised Manuscript Received March 31, 1989

ABSTRACT: In an effort to understand the nature of chromophore–protein interactions in bacteriorhodopsin (bR), we have reinvestigated dimethyl sulfoxide (DMSO)-induced changes in bR [Oesterhelt et al. (1973) *Eur. J. Biochem. 40*, 453–463]. We observe that dark-adapted bR (bR_{560}) in aqueous DMSO undergoes reversible transformation to a species absorbing maximally at 480 nm (bR_{480}). Beginning at 40% DMSO, this change results in complete conversion to bR_{480} at 60% DMSO. The kinetics of the reaction reveal that this transformation takes place predominantly through the all-trans isomeric form of the pigment. Thermal isomerization of the 13-cis chromophore to the all-trans form is, therefore, the rate-limiting step in the formation of bR_{480} from the dark-adapted bR. As in native bR, the chromophore in bR_{480} is linked to the protein via a protonated Schiff base, and its isomeric composition is predominantly all-trans. The formation of bR_{480} is associated with minor changes in the protein secondary structure, and the membrane retains crystallinity. These changes in the protein structure result in a diminished chromophore–protein interaction near the Schiff base region in bR_{480}. Thus, we attribute the observed spectroscopic changes in bR in DMSO to structural alteration of the protein. The 13-cis chromophoric pigment appears to be resistant to this solvent-induced change. The changes in the protein structure need not be very large; displacement of the protein counterion(s) to the Schiff base, resulting from minor changes in the protein structure, can produce the observed spectral shift.

Bacteriorhodopsin (bR), the only protein found in the purple membrane of the extreme halophile *Halobacterium halobium*, consists of retinal chromophore covalently bound to the protein by a Schiff base linkage to the ϵ-amino group of $lysine_{216}$. Upon absorbing light, the pigment undergoes a photocycle which is coupled to proton translocation across the cell membrane. It has a molecular weight of 26.5K, and its primary structure is known. The secondary structure shows considerable amount of α-helix. The helices form seven rodlike structures which span the membrane thickness and are oriented nearly perpendicular to its plane. The protein molecules are further arranged as cyclic trimers in a two-dimensional hexagonal lattice which results in a highly ordered rigid membrane structure [see e.g., Henderson (1977)]. Light-adapted bR (λ_{max} = 570 nm) contains the chromophore in the all-trans configuration. It decays with a half-life of ~25 min at room temperature to the stable dark-adapted form (λ_{max} = 560 nm) containing an equimolar mixture of the 13-cis and the all-trans isomers (Pettei et al., 1978).

The main factors governing the spectroscopic properties of retinal pigments are generally believed to be the protonation state of the Schiff base linkage between the chromophore and the protein and the spatial organization of the charged residues in the protein surrounding the chromophore [see, e.g., Honig and Ebrey (1982)]. Thus, chromophore–protein interactions play a key role in regulating the color of these pigments.

In an effort to understand the nature of the chromophore–protein interactions in bR and the determinants of its color, data on several low-wavelength-absorbing derivatives are summarized. When bR is regenerated from either the 13-*cis*- or the *all-trans*-retinal and bacterioopsin, an intermediate, absorbing maximally at ~440 nm, is formed in which the chromophore is apparently bound to the protein noncovalently (Schreckenbach et al., 1977, 1978). A ca. 440-nm-absorbing species is also observed when bR is solubilized in detergents (Konishi & Packer, 1977; London & Khorana, 1982). Indirect arguments are suggestive of a protonated Schiff base linkage between the chromophore and the protein in this derivative (Konishi & Packer, 1977). At pH above 11, native bR converts to a new form which absorbs maximally at ~460 nm and contains an unprotonated Schiff base linkage between the chromophore and the protein, as shown by resonance Raman spectroscopy (Drukmann et al., 1982). Baribeau and Boucher (1985) reported a 480-nm-absorbing species that forms upon solubilization of the delipidated bR in laurylsucrose at pH >7.5 (p*K* for the transition ~6.8). A 480-nm-absorbing species was also shown to result from the treatment of bR with volatile anesthetics (Nishimura et al., 1985). Quite recently, Brouillette et al. (1987) have also observed a ~480-nm bR species upon heating the native bR. By comparison of the observed absorption maxima with those of Drukmann et al. (1982), these groups inferred that their, respective, 480-nm-absorbing species contain an unprotonated Schiff base linkage between the chromophore and the protein.

bR undergoes some interesting changes in DMSO–water mixtures, and a thermodynamic equilibrium has been described (Oesterhelt et al., 1973) between bR_{560} and a species, the authors called the "460 nm complex" (λ_{max} around 460 nm), in mixtures containing 40–60% (vol %) DMSO. It was shown that, unlike the native bR_{560}, the 460-nm-absorbing species was reactive with hydroxylamine and borohydride.

We have reinvestigated the effect of DMSO–water mixtures on bR at 25 °C and show, in agreement with the earlier data (Oesterhelt et al., 1973), that in aqueous solutions of bR containing DMSO concentration above 40%, an equilibrium exists between bR_{560} and another species that absorbs maximally at ~480 nm, that we call bR_{480}. This equilibrium shifts

† This work was supported in part by National Institutes of Health Grant EYO 3142 (R.C.).

‡ City College of The City University of New York.

§ Permanent address: Biophysics Division, Clairol Research Laboratories, 2 Blachley Rd., Stamford, CT 06922.

∥ MRC Laboratory of Molecular Biology.

⊥ Universitätsspital.

Present address: Eye Research Institute, 20 Staniford St., Boston, MA 02114.

0006-2960/89/0428-5971$01.50/0

completely to bR_{480} at 60% DMSO. The absorption profile of bR_{480} is broad and has a marked shoulder at 460 nm. Even though our absorption spectrum of bR_{480} is identical with that reported earlier (Oesterhelt et al., 1973), they chose to call it the "460 nm absorbing species", presumably because its difference spectrum with bR_{560} has a maximum at 460 nm. Our kinetic data, however, in disagreement with the earlier work (Oesterhelt et al., 1973), suggest that the conversion from bR_{560} to bR_{480} takes place principally through the all-trans form of the pigment and the thermal isomerization about the C_{13}=C_{14} bond (i.e., converting the 13-cis pigment to the all-trans configuration) is indeed the rate-limiting step in this transformation. This scheme is substantiated by our chromophore extraction data which reveal that bR_{480} contains the chromophore in an all-trans configuration.

The chromophore in bR_{480} is shown to be bound to the protein by a protonated Schiff base linkage. Marked changes appear to take place in the Schiff base environment of bR_{560} upon formation of bR_{480}. Formation of bR_{480} is associated with slight changes in the protein secondary structure, and gross coformational changes are ruled out. The crystallinity of the molecules is maintained in bR_{480}.

Materials and Methods

Purple membrane prepared from *H. halobium* strain S-9 cells was a generous gift from Prof. Tom Ebrey. Dimethyl sulfoxide (99.9% pure, spectrophotometric grade) was obtained from Aldrich Chemical Co. and stored desiccated.

In order to avoid temperature fluctuations due to the large negative enthalpy associated with mixing DMSO and H_2O, bR_{480} was prepared by adding a concentrated sample of bR to a DMSO–H_2O mixture of the required concentration that had been equilibriated at 25 °C. For studying the effect of 60% DMSO on the light-adapted bR, the aqueous suspension of bR was first light-adapted with 568-nm or 530-nm light from a Kr^+ ion laser. The sample was then allowed to stand in the dark for about 0.5 min to allow all the photocycle intermediates to relax to the light-adapted bR (bR_{570}) form before making it 60% in DMSO, as described above.

The reversibility of the bR_{480} formation reaction was checked spectrophotometrically by diluting a solution of bR_{480} in 60% DMSO with water.

Absorption spectra were measured in a G. C. McPhearson spectrophotometer interfaced to a PDP-8 computer. The spectra were recorded at 24 ± 1 °C, with the bR concentrations typically ranging between 5 and 10 μM.

Resonance Raman spectra of bR_{480} were measured at 80 K using ~3 mW of a 457.9-nm line from an argon ion laser (Spectra Physics 165) as previously described (Pande et al., 1981). To obtain the resonance Raman spectrum of bR_{480}, the bR_{560} sample in 60% DMSO was allowed to completely convert to bR_{480} in the dark. Due to overwhelming fluorescence from bR_{480} at low temperature, the sample had to be concentrated by centrifugation at 20000*g* for 6 h, followed by suspension of the pellet in a minimum amount of the supernatent. Deuteriated bR_{480} sample was prepared by first deuteriating bR_{560} (Pande et al., 1981), followed by suspension in a 60% DMSO–D_2O mixture, monitoring its complete conversion to bR_{480} spectrophotometrically. The bR_{480} was then concentrated by centrifugation as described above. The sample was cooled very rapidly (<7 min) to 80 K, in order to avoid perturbation of the temperature-sensitive equilibrium between bR_{480} and bR_{560}. The nonnegligible solvent contribution to the Raman spectrum was removed by making parallel measurements on the solvent to subtract off the solvent lines from the composite spectra. The fluorescence contribution to the Raman spectra was removed as previously discussed (Pande et al., 1984).

A triplemate spectrometer (Spex Industries, Model 1877), connected to an LSI-11 computer (Digital Equipment Corp.) controlled OMA (optical multichannel analyzer) detector, was used to collect the Raman data. The OMA consists of a thermoelectrically cooled solid-state detector/controller assembly (EG&G Princeton Applied Research Model 1420-2/1218). The spectral resolution under our experimental conditions is about 8 cm^{-1}. The data were then calibrated against the Raman spectrum of toluene.

For the infrared spectrum, the suspension of bR_{480} was centrifuged in a desk-top centrifuge for 15–20 min until a clear supernatant was obtained. The resultant soft pellet was put as a drop in a CaF_2 cell with a 7-μm tin spacer. Infrared spectra were recorded in a Perkin-Elmer 983 scanning spectrometer, equipped with a Model 3600 data station for data acquisition and analysis. The spectrometer was continuously purged with dry air. Nine scans were recorded at a resolution of 3 cm^{-1} and signal-averaged from 2400 to 1100 cm^{-1}. The spectrum of 60% DMSO was also obtained under the same instrumental settings. This spectrum was subtracted from that of the sample spectrum such that the DMSO lines at 1317, 1406, and 1436 cm^{-1} were no longer visible in the resultant difference spectrum. For comparison, the spectrum of bR_{560} was recorded as partially dried film prepared by gently blowing dry air on a drop of concentrated solution of bR_{560} placed on a CaF_2 plate.

CD spectra were recorded in a JASCO J-40 AS spectropolarimeter. The protein concentration was about 25 μM, and the cell path length was 1 cm. The concentration of bR was obtained from the absorption spectrum using $\epsilon_{560} = 5.4 \times 10^4$ M^{-1} cm^{-1} for bR_{560}. For bR_{480}, ϵ_{480} was calculated to be 3.3×10^4 M^{-1} cm^{-1} from the absorption spectrum. Since a small amount (<5%) of bR remained in the native state, the concentration of bR_{480} used in CD studies is, correspondingly, slightly inaccurate. The base line using 60% DMSO was subtracted from the spectrum to obtain the final spectrum.

Chromophore chemical extraction was performed by denaturing the pigment using anhydrous ether and then passing it through a column of silica gel. Ether was quickly evaporated, and the sample was dissolved in an ether–hexane mixture (8:92). This was then passed through an HPLC system (Waters Associates) containing a 3-μm mesh silica column (10 cm × 0.3 cm) from IBM. The sample was eluted with an ether–hexane mixture (8:92), and the eluting fractions were monitored for their absorption at 360 nm. Dark- and light-adapted bR served as the necessary controls for this experiment.

X-ray analysis was carried out as follows. The specimen was centrifuged to form a pellet, then transferred to a glass capillary tube, packed into one end by further gentle centrifugation in a bench-top centrifuge, and finally flame-sealed to form a vacuum-tight specimen. X-ray photographs were obtained by using an Elliot toroidal focusing camera (Elliot, 1965). A thin capillary for the specimen and good collimation of the X-ray beam were needed because of the very high absorption of the X-ray beam by the 60% DMSO solution.

The bR used in these studies was unbuffered, and its intrinsic pH was ~6.5, prior to DMSO addition. Unless otherwise stated, all experiments were performed in the dark at 25 °C.

Results

The extinction coefficient of bR decreases almost linearly up to a concentration of ~40% upon adding increasing

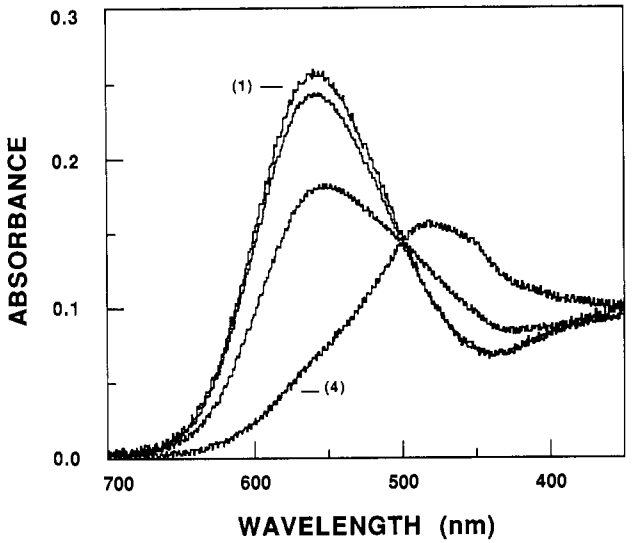

FIGURE 1: Changes in the absorption spectrum of bR as the concentration of DMSO in aqueous DMSO mixtures is increased at 25 °C. Spectra 1–4 represent DMSO concentrations of 35, 40, 50, and 60%, respectively. Measurements were made ~30 min after the DMSO concentration change. Spectrum 4 still shows residual absorption at ~550 nm because of the slow transformation rate to bR_{480} (see text).

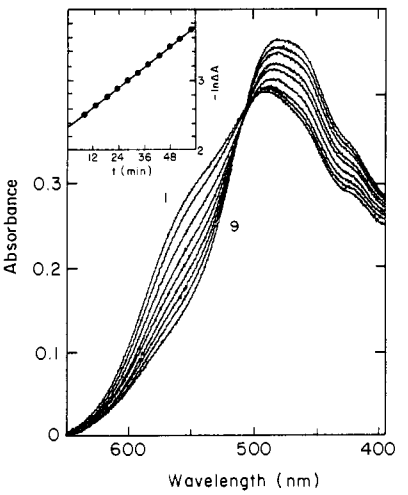

FIGURE 2: Time-dependent changes in the absorption spectrum of dark-adapted bR when an aqueous solution was made 60% in DMSO at 25 °C. Spectra 1–9 were measured at 2, 9, 23, 40, 63, 84, 119, 159, and 460 min, respectively, after the aqueous solution was made 60% in DMSO. The scan time was ~5 min over the entire wavelength range. The inset shows a log plot of the same reaction (but different set) monitored at 560 nm. The ordinate represents the log of the difference in the absorbance at any time (t) and that at infinite time (taken to be the value at ~6 h) after the reaction was started. The rate constant for this reaction was calculated to be 31 min from this plot.

amounts of DMSO to an aqueous solution of bR_{560} at 25 °C. Further increase in DMSO concentration results in the formation of a new species, bR_{480} (λ_{max} = 480 nm), in equilibrium with bR_{560}, as seen in Figure 1. This equilibrium shifts completely toward bR_{480} at 60% DMSO. These data are in good agreement with those reported earlier (Oesterhelt et al., 1973).

Time-dependent changes in the bR_{560} spectrum, following the increase in the DMSO concentration of an aqueous solution of bR to 60%, are shown in Figure 2. The inset is a log plot of the absorption changes with time; the linearity of the data demonstrates that the observed absorption changes are associated with a first-order process, the half-life for which was calculated to be 31 min from this plot. As is clear from this figure, the significant accumulation of bR_{480} seen in spectrum 1 cannot be accounted for by this rather slow rate and, therefore, must be the result of a faster process that was almost over by the time this spectrum was measured.

The light-adapted bR (bR_{570}) behaves very differently under the above experimental conditions; the reaction was complete by the time the second scan was made, with no change in the spectrum thereafter. In order to better estimate the rate of this relatively faster process, time-dependent changes were monitored at 570 nm after the light-adapted sample was made 60% in DMSO. The half-life of this reaction (data not shown) is <0.5 min.

Absence of the slow step in the kinetics of formation of bR_{480} from bR_{570} (an all-trans chromophoric pigment) pointed to the correspondence between this (slow) kinetic step and the presence of the 13-cis chromophoric pigment in bR_{560} (note that bR_{560} contains roughly an equimolar mixture of 13-cis and all-trans isomeric pigments). Since the kinetic data in Figure 2 could be fit to a single-exponential decay (see Figure 2, inset) and the spectral data show an isosbestic point, they represent a first-order conversion of the type A → B, where B represents the bR_{480} form. Spectrum 9 (last) in Figure 2 represents the spectrum due to pure "B" since it was recorded after a sufficiently long time to ensure completion of the process. Subtracting the appropriate contribution of this spectrum from any of the other composite spectra (1–8) containing contributions from "A" as well would yield the spectrum of pure "A" species. If our premise is correct, this spectrum should be the spectrum of 13-cis-containing bR. The spectrum thus obtained (not shown) has a maximum at 550 nm. This value, indeed, corresponds to the absorption maximum of bR containing only the 13-cis chromophore (Iwasa et al., 1981). Since bR_{560} contains an equimolar mixture of the 13-cis and the all-trans pigment forms, and the half-life for the transformation of the all-trans form to bR_{480} was found to be less than 0.5 min, we believe that the significant accumulation of bR_{480} observed at early times (spectrum 1, Figure 2) results from the all-trans pigment in bR_{560}. The ~31-min half-life calculated for the reaction in Figure 2 (inset) would then correspond to the transformation of the 13-cis pigment of bR_{560} to bR_{480} via the rate-limiting isomerization of the 13-cis to the all-trans isomeric form (see below).

In aqueous solution at room temperature, the all-trans to 13-cis thermal isomerization of bR (dark-adaptation) has a half-life of ~25 min and results in an equilibrium pigment population containing near equal amounts of the 13-cis and the all-trans isomeric forms. The half-life for thermal isomerization from the 13-cis to the all-trans form will, therefore, also be similar. If one assumes that the corresponding values in 60% DMSO may not be all that different, simple equilibrium considerations require a significant amount of thermal isomerization from the 13-cis to the all-trans isomeric form of the pigment during the slow phase (Figure 2), after the initial all-trans pigment has been converted to bR_{480}. Once formed, the all-trans pigment will convert to bR_{480} rapidly ($t_{1/2}$ < 0.5 min) as discussed above, which would lead to further 13-cis to all-trans isomerization. This reaction scheme

$$\underset{13\text{-cis}}{bR_{560}} \rightleftharpoons \underset{\text{all-trans}}{} \xrightleftharpoons{40\text{-}60\%\ \text{DMSO}} \underset{\text{all-trans}}{bR_{480}}$$

which makes the thermal isomerization of the 13-cis pigment to the all-trans form the rate-limiting step in the bR_{560} to bR_{480} transformation, requires that the bR_{480} formed, either from

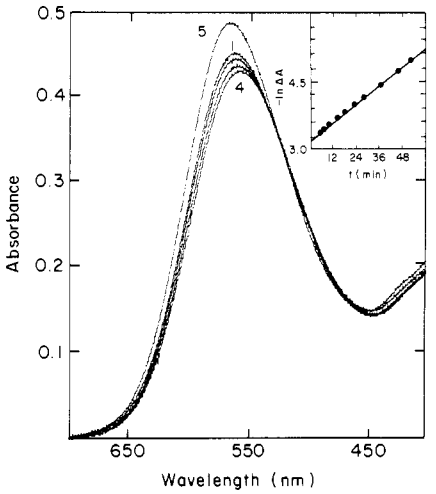

FIGURE 3: Time-dependent changes in the absorption spectrum of the purple complex, which resulted upon dilution of bR_{480}, originally formed from the dark-adapted bR. The initial fast reaction, that formed the purple complex, could not be resolved in our system and was over in under a minute. The final DMSO concentration of the sample, after dilution, was ~20%. Spectra 1–4 were measured at 2, 9, 34, and 108 min, respectively, after dilution. The scan time was ~5 min over the entire wavelength range. Spectrum 5 was obtained by irradiating the sample, represented by spectrum 4, using 530-nm light under conditions used for the light adaptation of the native bR. The inset shows the log plot of the reaction represented by spectra 1–4, but in a different set. The absorbance changes were measured at 586 nm, which corresponds to the maxima in the difference spectrum between the light- and the dark-adapted bR. The ordinate represents the log of the difference in the absorbance of the sample at time t and that after 2 h. The half-life for this reaction was calculated to be 22 min from this plot.

the light- or from the dark-adapted bR, should have the chromophore exclusively in the all-trans isomeric form. Provided the thermal isomerization of bR_{480} is slow (which it is, see below), reversal of the above reaction by dilution should, therefore, result in the formation of bR with the chromophore exclusively in the all-trans form (light-adapted), regardless of whether the bR_{480} originated from bR_{560} or bR_{570}.

The result of such an experiment with bR_{480}, originally prepared from the dark-adapted bR(bR_{560}), is shown in Figure 3 and is, indeed, in accordance with the above proposed scheme. A relatively fast reaction, resulting in the formation of purple complex following the dilution of bR_{480}, could not be resolved. This reaction was over by the time the first spectrum was measured (~2 min). Spectra 1–4 represent the time-dependent changes in bR following its fast initial formation. No further time-dependent changes beyond spectrum 4 were observed in the sample. This sample was then light-adapted with 530-nm light, and the resulting absorption is shown as spectrum 5. Complete dark adaptation of this light-adapted sample resulted in a spectrum which was indistinguishable from spectrum 4. Furthermore, the kinetics of this dark adaptation were identical with the time-dependent changes typified by spectra 1–4; both follow a first-order process (Figure 3, inset) with a half-life of ~22 min, which is similar to the dark adaptation rate for the native bR. These observations clearly demonstrate that the dilution of bR_{480} results in the formation of bR which is significantly light-adapted. Since spectrum 4 represents completely dark-adapted bR (equimolar mixture of the 13-cis and all-trans isomeric pigments), while spectrum 5 represents completely light-adapted bR (100% all-trans pigment), we calculate from spectrum 1 that the bR formed upon dilution of bR_{480} contains ~70% of the pigment in the all-trans isomeric form. Furthermore, since the dilution was performed before all the bR_{560} had transformed to bR_{480}, we estimate that the correction for the 13-cis contribution from the untransformed bR_{560} will increase the amount of the all-trans species to ~80% in the regenerated bR. Under similar conditions, bR_{480} obtained from light-adapted bR (data not shown) yielded ~85% all-trans pigment. These data are in good agreement with the above reaction scheme and suggest that the thermal isomerization of the 13-cis to the all-trans isomeric form of the pigment is, indeed, the rate-limiting step in the conversion of bR_{560} to bR_{480}.

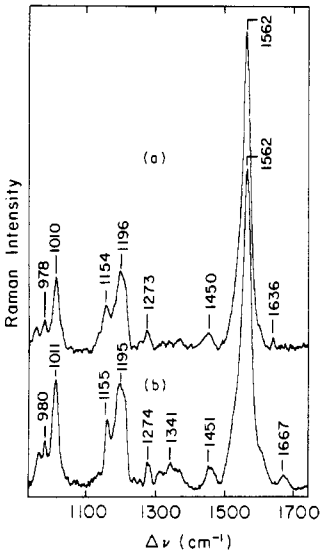

FIGURE 4: Resonance Raman spectra of bR_{480} in D_2O (a) and H_2O (b) at 80 K. The spectra were probed with ~3 mW of 457.9-nm light from an Ar^+ laser. The solvent contribution to the Raman spectra has been subtracted out.

Our chromophore extraction data reveal that bR_{480}, obtained from bR_{560}, contains ~85% all-trans and ~15% 13-cis isomeric form of the chromophore, in complete agreement with the deduction based on the absorption data. Furthermore, the isomeric composition of bR_{480} did not change upon standing at room temperature up to 22 h, the longest time tested, suggesting that, unlike bR, the chromophore of bR_{480} does not undergo thermal isomerization (dark adaptation).

Figure 4 compares the resonance Raman spectra of bR_{480} in H_2O and D_2O. The Schiff base peak at 1667 cm^{-1} in H_2O solution (Figure 4b) shifts to 1636 cm^{-1} upon deuteriation (Figure 4a). These data unequivocally show that, as in the native bR, the chromophore in bR_{480} is linked to the protein via a protonated Schiff base. The Schiff base position, as well as its shift upon deuteriation, is quite different from those observed for bR_{560}. These will be discussed in detail below. The absence of any significant Raman signal at ~1530 cm^{-1}, the expected peak position for the dominant ethylenic line of bR_{560} (Aton et al., 1977), suggests that the rapid cooling of the sample prevented significant perturbation of this temperature-sensitive pigment equilibrium (Oesterhelt et al., 1973). The observed Raman spectrum, therefore, represents the vibrational modes entirely due to bR_{480}.

The fingerprint region in the resonance Raman spectrum, besides being sensitive to the geometry of the chromophore, is also sensitive to protein–chromophore interactions. Comparison with the bR_{560} spectrum (Aton et al., 1977) reveals that marked changes take place in this region as well, upon bR_{480} formation. Furthermore, the bR_{480} spectrum in this region shows significant similarities with the spectrum of the all-trans-protonated Schiff base of retinal (Pande et al., 1981), despite a somewhat lower frequency for the low-frequency

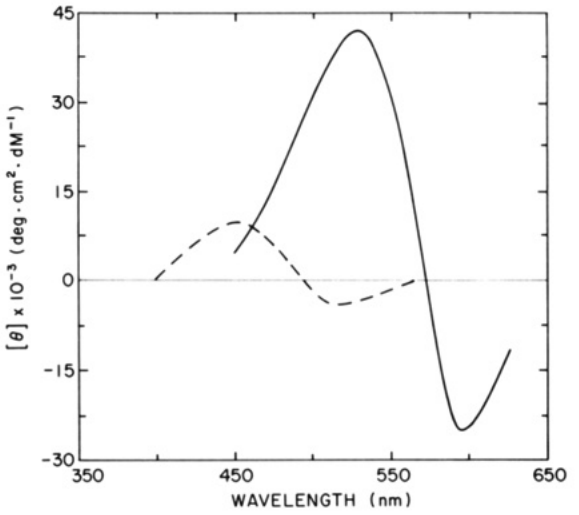

FIGURE 5: CD spectrum of bR_{560} (solid line) and bR_{480} (dashed line). The spectra were measured in a 1-cm path-length cell. The sample concentration was typically 25 μM. Base-line correction was made by using water and 60% DMSO for the bR_{560} and bR_{480}, respectively, to obtain the final spectra.

mode (1154 cm^{-1} compared to 1164 cm^{-1}). These results are in agreement with the deduction, based on the absorption and the chromophore extraction data, that the chromophore in bR_{480} is predominantly in the all-trans isomeric form.

The trimeric structure of bR is characterized by exciton bands in the visible CD spectrum [see, e.g., Ebrey et al. (1977)]. Since these bands arise due to exciton exchange between the neighboring molecules in an ordered, periodic structure, they are very sensitive to structural changes. In order to compare the structure of bR_{480} with that of the native bR in this regard, we have measured the visible CD spectrum of bR_{480}. The data in Figure 5 show that in keeping with the lower (hypsochromic) λ_{max} of bR_{480}, compared to the native bR, the exciton CD bands and the crossover point have correspondingly shifted to lower wavelengths. The exciton bands are, however, weaker in intensity than in the native bR. Although the extinction coefficient of bR_{480} is smaller than that of bR_{560} by a factor of 1.6, the exciton bands of bR_{480} are at least 5 times smaller than those of bR_{560}. This difference cannot solely be due to the smaller extinction coefficient of bR_{480}. A variety of reasons can be responsible for the decrease in the rotatory strength. For example, a change in the angle between the transition dipole moments of the interacting chromophores due to a slight change in the chromophore–protein interaction of the individual pigment molecules can change the exciton interaction. Also, formation of dimers, at the expense of trimers, can decrease the size of these bands (Ebrey et al., 1977). It should be noted that these results are in contradiction to an earlier report (Heyn et al., 1975) in which the exciton coupling was reported lost upon the formation of bR_{480}.

Conclusions regarding the bR_{480} structure based on our CD data are supported by our X-ray measurements shown in Figure 6. The concentric rings seen in this plate are similar to those observed in native purple membrane, where they arise from the periodic structure of bR molecules packed into a p3 lattice [see e.g., Henderson (1977)]. Closer observation, however, reveals that, compared to the native membrane where the rings are sharp and strong, the rings in the bR_{480}-containing membrane are somewhat diffuse and may also be weaker with a possibility of a difference in the distribution of intensity. However, these last two points are less certain: the apparent weakness in the rings may be a consequence of the high absorption by DMSO, and the exact pattern of diffraction intensity is not easy to distinguish when the rings are somewhat diffuse. Furthermore, there is a possible ambiguity in an unoriented specimen with somewhat diffuse rings: some of the rings may arise from diffraction perpendicular to the membrane planes if there is any tendency to stacking of the membranes in the pellet. There is no doubt, however, that there is a lattice of bR molecules present either having cell dimensions that are a bit variable or consisting of small patches containing only a few (50–100) molecules. Given that there are now three well-studied two-dimensional crystal structures having an identical structure at 6-Å resolution (Tsygannik & Baldwin, 1987; Leifer & Henderson, 1983; Unwin & Henderson, 1975) and given the similarity of Figure 6 to that of native, it is likely that the bR strucure in 60% DMSO is not grossly different from the native. In an earlier, unpublished, study of purple membrane referred to as a private communication in Heyn et al. (1975), one of the authors (R.H.) concluded that the rings from the surface lattice had disappeared in 60% DMSO. The present photograph in Figure 6 shows this is not true and was overlooked then because of the high absorption of the DMSO itself, together with the diffuse and perhaps weaker nature of the diffraction. The present study, properly documented, shows that there is indeed a lattice of some kind, though an exact description of its nature cannot be given without further experiment.

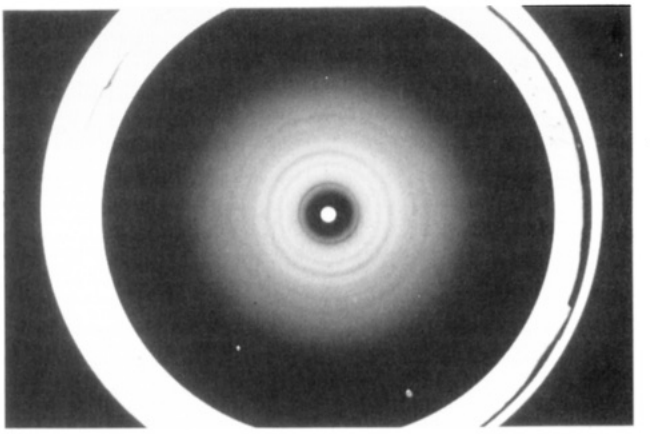

FIGURE 6: Diffraction pattern from a thin specimen of bR_{480}. The X-ray beam passed through an unoriented pellet of the membrane and was masked off so that only the sample was allowed to contribute to the diffraction pattern. This was necessary because of the very high absorption of X-rays by the 60% DMSO solution.

The region between 1000 and 1800 cm^{-1} in the IR spectrum of proteins contains vibrational bands from the peptide bonds of the protein backbone and yields information on the protein secondary structure. However, it is difficult to measure the spectrum of bR_{480} in this region because both DMSO and water absorb around 1650 cm^{-1} and DMSO has several bands in the spectral region between 1700 and 1000 cm^{-1}. Subtraction of the contributions due to DMSO and water (solvent) gives a rather noisy spectrum. Therefore, only the more intense amide I and II region is shown in Figure 7b. For comparison, the spectrum from bR_{560} in the same region has also been included (Figure 7a). The bR_{480} spectrum is only slightly, but significantly, different from the bR_{560} spectrum; the amide I band at 1665 cm^{-1} is narrow and symmetric compared to the rather broad asymmetric band of bR_{560} which is centered at 1660 cm^{-1} and has shoulders at 1689 and 1639 cm^{-1}. There are, however, no observable differences between the amide II bands of the two species. bR is predominantly α-helical; the presence of β-sheet structure has often been suggested but still remains controversial [see Rothschild (1988) and references

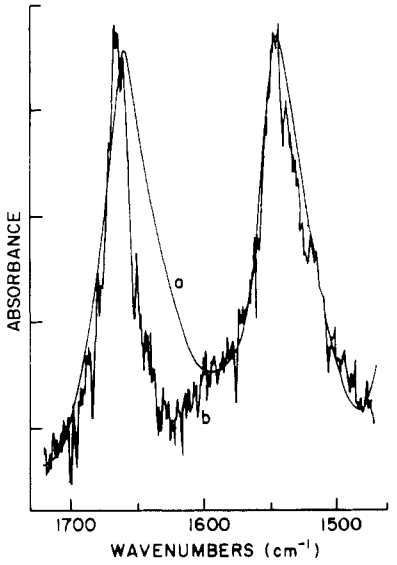

FIGURE 7: IR spectrum of native bR (a) and bR_{480} (b). In the case of bR_{480}, due to strong absorption from DMSO in this spectral region, the solvent contribution to the sample spectrum was removed by subtracting off the spectrum of the solvent (taken separately) until the solvent-specific peaks reduced to zero intensity. This results in a weaker (relatively poor signal/noise ratio) contribution from bR_{480}.

cited therein]. The 1639 cm^{-1} shoulder, which, despite the poor signal (Figure 7b), is clearly absent in the spectrum of bR_{480}, is considered a marker for the β-sheet structure. On this basis, it would appear that the formation of bR_{480} results in the loss of this β-sheet structure.

Increase in the DMSO concentration from 60% to 70% in aqueous solutions of bR results in the irreversible formation of a new species with the absorbance maximum at ~390 nm. The transformation shows a clear isosbestic point (data not shown). Data analysis reveals that the decrease in absorbance at 480 nm represents a first-order process with a half-life of 3.6 h. Recently, Brouillette et al. (1987) have also observed an irreversible shift in the absorption of bR to ~370 nm upon heating.

Discussion

Our absorption studies suggest that the rate-determining step in the conversion of bR_{560} to bR_{480} involves thermal isomerization of the 13-cis to the all-trans form. Our conclusion is in contradiction with the earlier published work of Oesterhelt et al. (1973). One of the reasons for this apparent discrepancy lies in their observation of 13-*cis*-retinal in thin-layer chromatograms of bR in DMSO. This result is confusing, and it leads to their incorrect interpretation of the temperature-jump data (their Figure 5b); they suggest that the kinetics refer to the *dissociation* of the purple complex to bR_{480} when, in fact, it refers to its *formation*. The zero-time extrapolated values, in their case, actually represent the ratio of the contributing pigment forms in bR_{480}. These data, which could be compared to our dilution experiment (Figure 3), are in agreement with our observation and suggest the predominance of one isomeric form in bR_{480}, which we have shown to be the all-trans form. Oesterhelt et al. (1973), in their hydroxylamine reaction, did see a fast initial phase, after which only the purple complex was left, followed by a slow linear phase, which took ~2 h to complete. We believe that these two rates correspond to the rates we observe in the biphasic transformation of bR_{560} and attribute them to the conversion of the all-trans pigment to bR_{480} and the rate-limiting thermal isomerization of the 13-cis to the all-trans pigment form.

Our resonance Raman data clearly show that the Schiff base linkage in bR_{480} is protonated. There are some other subtle features in these spectra that need discussion. The C=N stretching mode in bR_{480} appears at 1667 cm^{-1} which is unusually high when compared to the native bR (1642 cm^{-1}), and shows a large shift of 31 cm^{-1} upon deuteriation. The C=N stretching frequency and also its shift upon deuteriation are independent indexes of the Schiff base environment [e.g., see Kakitani et al. (1983)]. This sensitivity derives from a coupling between the C=N stretch and the C=N—H bending modes. Since a protein counterion is believed to interact with the Schiff base in visual pigments and bR [see Honig and Ebrey (1982) and references cited therein], this mode would be expected to be very sensitive to the magnitude of this interaction and the hydrogen-bonding environment of the Schiff base nitrogen (Gilson et al., 1988). For bR and its photointermediates which have a protonated Schiff base, the deuteriation shifts are usually small, about 17 cm^{-1}, whereas bovine rhodopsin and its intermediates show relatively larger deuterium isotope shifts. These results have been interpreted as suggestive of a weaker hydrogen-bonding interaction between the protein counterion in bR and its photointermediates, compared to the visual pigments. Thus, it is remarkable that the resonance Raman spectrum of bR_{480} shows strong similarities to the Schiff base region of the protonated Schiff bases of the model compounds (PSBs). For comparison, the all-trans PSB in ethanol has the C=N stretching frequency at 1661 cm^{-1} which shifts by 30 cm^{-1} upon deuteriation (Pande et al., 1981). These relatively high frequencies for the C=N stretch, and their shift upon deuteriation in acidified ethanol solutions, result from the strong interaction between the protonated Schiff base and its counterion (Cl^-) in solution. Electrically neutral solvent dipoles can also interact with the protonated Schiff bases of retinal and, in some cases, as in methanol, produce a larger effect on the C=N stretching frequency and its shift upon deuteriation, compared to an anion (Gilson et al., 1988).

The close similarity in the properties of the C=N vibrational mode of the PSB and the bR_{480} species suggests that the protonated Schiff base of the protein-bound chromophore interacts very strongly with the counterion. This can result from the replacement of the protein counterion with an anion in solution, or solvent dipole, due to the opening up (solvent permeation) of the chromophore binding site. It has been shown by Oesterhelt et al. (1973) that bR_{480}, in contrast to the native bR, reacts with hydroxylamine as well as borohydride in the dark. Their data suggest that the formation of bR_{480} results in the exposure of the Schiff base to the solvent, presumably due to a protein structural change. In fact, DMSO at these and higher concentrations has been shown to cause structural changes in proteins and synthetic homopolymers of selected amino acids (Hamaguchi, 1964; Glickson et al., 1972; Bradbury et al., 1972; Jacobson & Krueger, 1975; Jacobson & Turner, 1980). Thus, we believe that the hyposochromic shift in the absorption maximum of bR_{480}, as well as the observed properties of the C=N stretching mode, results from the replacement of the protein counterion of the protonated Schiff base with the solvent dipole(s), since we do not expect significant anions under our experimental conditions. This would also be consistent with a much higher C=N stretch, even compared to PSB (1667 cm^{-1}, compared to 1661 cm^{-1} for PSB in methanol), since DMSO is a very strong hydrogen-bond acceptor (see below).

A number of physical properties of water–DMSO, or solvent systems containing water with other organic cosolvent, show

a sharp transition as a function of the solvent composition. This change usually signifies change in the water structure from the highly associated state to a less ordered state (Lumrey & Rajender, 1970). Indeed, it has been suggested that DMSO is a better hydrogen-bond acceptor than water, and, therefore, beyond a critical concentration in aqueous solutions, it will affect the water structure (Kharash & Thyagarajan, 1983). For the water–DMSO system, this transition occurs at ~30 mol % of DMSO (or ~60% v/v) (MacDonald & Heyn, 1970; Glickson et al., 1972). The free energy of any protein structure in solution will have contributions from both the intramolecular interactions and also the solute–solvent interactions. Perhaps it is not very surprising, then, that a change in the solvent properties will reflect as a change in the intramolecular interactions (in the form of a rearrangement in the protein structure to offset the change in the energetics of the solute–solvent forces). For a membrane-bound protein like bR, the changes in the secondary structure can occur directly in the extramembranous regions that are in contact with the solvent, or they can be transmitted to the transmembranous regions through these exposed residues. The possibility that DMSO, due to its strong hydrogen-bond acceptor properties, directly affects the hydrogen bonding in the protein, and therefore its structure, cannot be ruled out from our data.

It has been reported (Spudich et al., 1986; Rodman et al., 1986; Lugtenburg et al., 1986) that the 3500 cm^{-1} "opsin shift" (the difference in the λ_{max} between the pigment and the protonated Schiff base of the corresponding retinal with *n*-butylamine in methanol, expressed in cm^{-1}), out of a total of 5100 cm^{-1}, observed in bR is associated with the interactions near the Schiff base end of the chromophore, while the remainder is attributed to a combination of ring-chain planarization as well as to the ion pair in the β-ionone portion of the chromophore. As discussed above, our Raman data show that the formation of bR_{480} results in significant changes in the Schiff base environment, presumably due to a perturbation in the protein–chromophore interaction in this region. A complete loss of such interactions in this region [replacement of the protein counterion with the solvent dipole(s)] should, therefore, result in a ca. 3500 cm^{-1} loss in the "opsin shift" of bR_{560} upon formation of bR_{480}. Our data show that the formation of bR_{480}, indeed, results in ~80-nm (~3000 cm^{-1}) blue shift, which is in good agreement with the calculated value.

It should be noted that the proposed changes in the Schiff base region, resulting in the formation of bR_{480}, do not require gross structural changes in the protein structure and may derive from small localized changes, which would be beyond the resolution of the current X-ray techniques. In fact, our X-ray (Figure 6) as well as CD (Figure 5) studies in the visible region show that crystallinity of the membrane is maintained in bR_{480} too, thus arguing against any gross protein structural change. The IR data suggest subtle changes in the protein secondary structure, and these changes, very likely, are responsible for the displacement of the protein counterion, resulting in the observed blue-shift in the absorption maximum.

The irreversible formation of bR_{390} upon increasing the DMSO concentration to 70% DMSO, by analogy to the meta I to meta II conversion in visual pigments, presumably results from the deprotonation of the Schiff base [cf. Doukas et al. (1978) and references cited therein]. Since the absorption maximum of the *all-trans*-retinal in 70% DMSO is also at ~391 nm, bR_{390} could also represent free retinal resulting from the hydrolysis of the chromophore–protein Schiff base linkage. At present, we cannot distinguish between these two possibilities.

In conclusion, our studies indicate that in aqueous DMSO solutions containing >35% (v/v) DMSO, bR exists in two distinctly different states corresponding to bR_{560} and bR_{480}. The transition between these two forms appears to be energetically coupled to the changes in the solvent structure, with the higher DMSO concentration favoring the more "open" bR_{480} form. The two forms appear to have some subtle differences in the protein structure rather than gross differences in folding. The isomeric state of the chromophore appears to act as a "switch" for this transformation, the conversion taking place predominantly through the all-trans pigment form while the 13-cis form is resistant to this change. The hypsochromic shift in the absorption maximum of the native bR, accompanying the formation of bR_{480}, does not result from the deprotonation of the Schiff base. Loss of specific chromophore–protein interactions, especially in the Schiff base region, appears to be responsible. Thus, specific chromophore–protein interactions are responsible, not only for the color of bR but also for its stability.

ACKNOWLEDGMENTS

We thank Dr. V. J. Rao for his help with the chromophore extractions.

REFERENCES

Aton, B., Doukas, A. G., Callender, R. H., Becher, B., & Ebrey, T. G. (1977) *Biochemistry 16*, 2995–2999.
Baribeau, J., & Boucher, F. (1985) *Can. J. Biochem. Cell. Biol. 63*, 305–312.
Becher, B., & Cassim, J. (1975) *Prep. Biochem. 5*, 161–178.
Bradbury, E. M., Crane-Robinson, C., Giancotti, V., & Stephens, R. M. (1972) *Polymer 13*, 33–39.
Brouillette, C. G., Muccio, D. D., & Finney, T. K. (1987) *Biochemistry 26*, 7431–7438.
Doukas, A. G., Aton, B., Callender, R. H., & Ebrey, T. (1978) *Biochemistry 17*, 2430–2435.
Drukmann, S., Ottolenghi, M., Pande, A., Pande, J., & Callender, R. H. (1982) *Biochemistry 21*, 4953–4959.
Ebrey, T. G., Becher, B., Mao, B., Kilbride, P., & Honig, B. (1977) *J. Mol. Biol. 112*, 377–397.
Elliot, A. (1965) *J. Sci. Instrum. 42*, 312–316.
Gilson, H. S. R., Honig, B., Croteau, A., Zarrilli, G., & Nakanishi, K. (1988) *Biophys. J. 53*, 261–269.
Glickson, J. D., Urry, D. W., & Roderich, W. (1972) *Proc. Natl. Acad. Sci. U.S.A. 9*, 2566–2569.
Hamaguchi, K. (1964) *J. Biochem. (Tokyo) 56*, 441–449.
Henderson, R. (1977) *Annu. Rev. Biophys. Bioeng. 6*, 87–109.
Heyn, M., Bauer, P., & Dencher, N. (1975) *Biochem. Biophys. Res. Commun. 67*, 897–903.
Honig, B., & Ebrey, T. (1982) *Methods Enzymol. 88*, 462–470.
Iwasa, T., Tokunaga, F., & Yoshizawa, T. (1981) *Photochem. Photobiol. 33*, 539–545.
Jacobson, A. L., & Krueger, P. J. (1975) *Biochim. Biophys. Acta 393*, 274–283.
Jacobson, A. L., & Turner, C. L. (1980) *Biochemistry 19*, 4534–4538.
Kakitani, H., Kakitani, Y., Rodman, H., Honig, B., & Callender, R. (1983) *J. Phys. Chem. 87*, 3620–3628.
Kharasch, N., & Thyagarajan, B. S. (1983) *Ann. N.Y. Acad. Sci. 411*, 391–402.
Konishi, T., & Packer, L. (1977) *FEBS Lett. 79*, 369–373.
Leifer, D., & Henderson, R. (1983) *J. Mol. Biol. 163*, 451–466.
London, E., & Khorana, H. G. (1982) *J. Biol. Chem. 257*, 7003–7011.

Lumrey, R., & Rajender, S. (1970) *Biopolymers 9*, 1125-1227.
Nishimura, S., Mashimo, T., Hiraki, K., Hamanaka, T., Kito, Y., & Yoshiya, I. (1985) *Biochim. Biophys. Acta 818*, 421-424.
Oesterhelt, D., Meentzen, M., & Schuhmann, L. (1973) *Eur. J. Biochem. 40*, 453-463.
Pande, J., Callender, R. H., & Ebrey, T. G. (1981) *Proc. Natl. Acad. Sci. U.S.A. 78*, 7379-7382.
Pande, A., Callender, R., Ebrey, T., & Tsuda, M. (1984) *Biophys. J. 45*, 573-576.
Pettei, M., Yudd, A. P., Nakanishi, K., Henselman, R., & Stoeckenius, W. (1977) *Biochemistry 16*, 1955-1958.
Rothschild, K. J. (1988) *Photochem. Photobiol. 47*, 883-887.
Schreckenbach, T., Walckhoff, B., & Oesterhelt, D. (1977) *Eur. J. Biochem. 6*, 499-511.
Schreckenbach, T., Walckhoff, B., & Oesterhelt, D. (1978) *Biochemistry 17*, 5353-5359.
Spudich, J., McCaine, D. A., Nakanishi, K., Okabe, M., Shimizu, N., Rodman, H., Honig, B., & Bogomolni, R. (1986) *Biophys. J. 49*, 479-483.
Tsygannik, I. N., & Baldwin, J. M. (1987) *Eur. Biophys. J. 14*, 263-272.
Unwin, P. N. T., & Henderson, R. (1975) *J. Mol. Biol. 94*, 425-440.

Analysis of the Relative Contributions of the Nuclear Overhauser Interproton Distance Restraints and the Empirical Energy Function in the Calculation of Oligonucleotide Structures Using Restrained Molecular Dynamics†

Angela M. Gronenborn* and G. Marius Clore*
Laboratory of Chemical Physics, Building 2, National Institute of Diabetes and Digestive and Kidney Diseases, National Institutes of Health, Bethesda, Maryland 20892
Received February 21, 1989; Revised Manuscript Received April 5, 1989

ABSTRACT: The relative contributions of the interproton distance restraints derived from nuclear Overhauser enhancement measurements and of the empirical energy function in the determination of oligonucleotide structures by restrained molecular dynamics are investigated. The calculations are based on 102 intraresidue and 126 interresidue interproton distance restraints derived from short mixing time two-dimensional nuclear Overhauser enhancement data on the dodecamer 5'd(CGCGPATTCGCG)$_2$ [Clore, G. M., Oschkinat, H., McLaughlin, L. W., Benseler, F., Scalfi Happ, C., Happ, E., & Gronenborn, A. M. (1988) *Biochemistry 27*, 4185-4197]. Eight interproton distance restraint lists were made up with errors ranging from $-0.1/+0.2$ to $-1.2/+1.3$ Å for $r < 2.5$ Å and from $-0.2/+0.3$ to $-1.3/+1.4$ Å for $r \geq 2.5$ Å. These restraints were incorporated into the total energy function of the system in the form of square-well potentials with force constants set sufficiently high to ensure that the deviations between calculated distances and experimental restraints were very small (average interproton distance rms deviation of less than 0.06 Å). For each data set, six calculations were carried out, three starting from classical A-DNA and three from classical B-DNA. The results show that structural changes occurring during the course of restrained molecular dynamics and the degree of structural convergence are determined by the interproton distance restraints. All the structures display similar small deviations from idealized geometry and have the same values for the nonbonding energy terms comprising van der Waals, electrostatic, and hydrogen-bonding components. Thus, the function of the empirical energy function is to maintain near perfect stereochemistry and nonbonded interactions. Local structural variations can be determined up to error limits of $-0.2/+0.3$ Å for $r < 2.5$ Å and $-0.3/+0.4$ Å for $r \geq 2.5$ Å. Up to error limits of $-0.4/+0.5$ Å for $r < 2.5$ Å and $-0.5/+0.6$ Å for $r \geq 2.5$ Å local structural variations are still discernible, although the spread of the structures becomes appreciably larger. For larger error limits local structural variations cannot be assessed at all.

Over the last few years considerable success has been achieved in determining three-dimensional structures of macromolecules in solution by nuclear magnetic resonance (NMR)[1] spectroscopy on the basis of NOE-derived interproton distance restraints [see Wüthrich (1986, 1989) and Clore and Gronenborn (1987, 1989) for reviews]. While the application of this methodology in the case of proteins has now been widely accepted, there has been some dispute regarding its application to oligonucleotides. This has arisen in part because the distance restraints for oligonucleotides are limited to adjacent base pairs so that, unlike in proteins, there are no tertiary NOE restraints to position non nearest neighbors with respect to each other. There have been essentially two schools of thought. The first has made use of metric matrix distance geometry calculations and has asserted that as the algorithm uses exclusively distance information the resulting structures are determined solely from the experimental distance restraints (Hare & Reid, 1986; Hare et al., 1986a,b; Reid, 1987; Patel et al., 1987; Nerdal et al., 1988; Pardi et al., 1988). The second

† This work was supported by the Intramural AIDS Anti-Viral Targeted Program of the Office of the Director of the National Institutes of Health.

[1] Abbreviations: NMR, nuclear magnetic resonance; NOE, nuclear Overhauser effect; RD, restrained dynamics; rms, root mean square.